

# NJC

Accepted Manuscript



This is an *Accepted Manuscript*, which has been through the Royal Society of Chemistry peer review process and has been accepted for publication.

*Accepted Manuscripts* are published online shortly after acceptance, before technical editing, formatting and proof reading. Using this free service, authors can make their results available to the community, in citable form, before we publish the edited article. We will replace this *Accepted Manuscript* with the edited and formatted *Advance Article* as soon as it is available.

You can find more information about *Accepted Manuscripts* in the [Information for Authors](#).

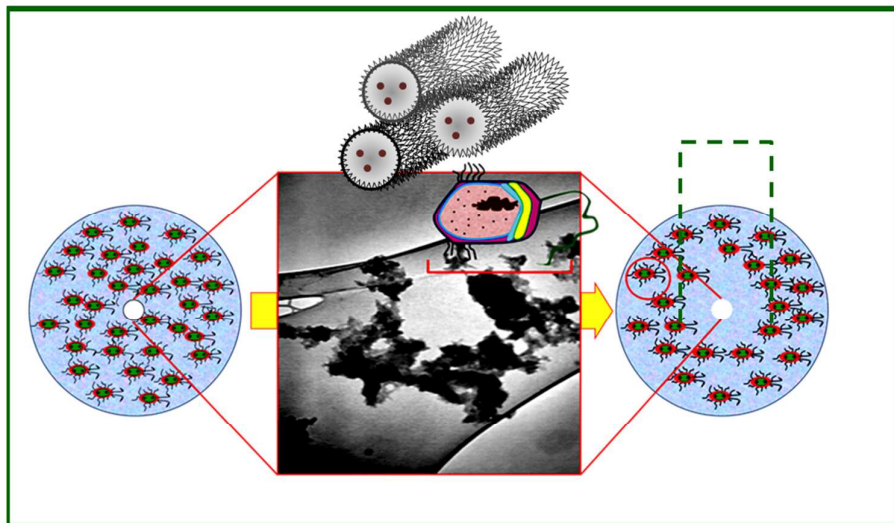
Please note that technical editing may introduce minor changes to the text and/or graphics, which may alter content. The journal's standard [Terms & Conditions](#) and the [Ethical guidelines](#) still apply. In no event shall the Royal Society of Chemistry be held responsible for any errors or omissions in this *Accepted Manuscript* or any consequences arising from the use of any information it contains.



[www.rsc.org/njc](http://www.rsc.org/njc)

## Graphical Abstract

Antibacterial effect of a nanotube shaped PPy-Pd composite



# Novel nanotube-shaped polypyrrole-Pd composite prepared using reverse microemulsion polymerization and its evaluation as an antibacterial agent

Alireza Salabat<sup>\*,a</sup>, Farid Mirhoseini<sup>a</sup>, Majid Mahdih<sup>b</sup> and Hassan Saydi<sup>a</sup>

<sup>a</sup> Department of Chemistry, Faculty of Science, Arak University, 38156-8-8349, Arak, Iran

<sup>b</sup> Department of Biology, Faculty of Science, Arak University, 38156-8-8349, Arak, Iran

\* Correspondence to: A. Salabat, TEL: +98-86-34173400; Fax: +98-86-34173406;

E-mail address: [A-Salabat@araku.ac.ir](mailto:A-Salabat@araku.ac.ir)

## Abstract

Due to huge number of applications of polymer-noble metal nanocomposite, a simple synthesis route for the design of polypyrrole nanotubes in the presence of Pd nanoparticles (PPy-Pd) has been reported in this paper. In this method synthesized Pd nanoparticles using rosemary extract, as reducing agent, combined with a reverse cylindrical micelle containing pyrrole monomer and an aqueous FeCl<sub>3</sub> solution to produce nanotube-shaped PPy-Pd composite. The synthesized nanotube PPy-Pd composite was studied using different characterization techniques such as FTIR, XRD, SEM and TEM. The antibacterial activity of the synthesized nanocomposite was evaluated against clinical isolates of Gram-positive (*Bacillus spp.* and *Staphylococcus aureus*) and Gram-negative (*Escherichia coli* and *Klebsiella spp.*) bacteria. The Kirby-bauer method for determination of inhibition zone and micro-plate dilution method for investigation of Minimal Inhibitory Concentration (MIC) and Minimal Bactericidal Concentration (MBC) were accomplished. The obtained results exhibited that antibacterial activity of the nanocomposite was improved compared with pure polypyrrole due to existence of Pd nanoparticles.

**Keywords** Polypyrrole; Nanotube; Nanocomposite; Pyrrole; Microemulsion system; Rosemary extract, Antibacterial activity

## 1. Introduction

Polymer nanocomposites containing noble metals have been gained tremendous attention

in a wide range of applications due to their versatility, and tunable characteristics including physical, chemical and mechanical properties.<sup>1,2</sup>

Fabrication of the nanocomposites with tubular nanostructure, that are one dimensional nanostructure, is quite difficult compared with spheres, rods, and fibers structures. It is known that the various nanotubes have been made of carbon, ceramics, metals, polymers, and so forth. The idea in this research is fabrication of a tubular nanostructure of polymer-metal nanocomposite using a soft template synthesis and green chemistry approach. Recently, intrinsic conducting polymers with conjugated double bonds such as polypyrrole (PPy) have played indispensable roles in specialized industrial applications due to its easy synthesis, good environmental stability, electrical conductivity, reversible electrochemical behavior, optical properties and so forth.<sup>3,4</sup> On the other hand, transition metal nanoparticles of silver, gold, platinum and palladium provide new opportunities for the remarkable enhancement in the biological and chemical process due to their unique electronic, optical, and magnetic properties.<sup>5-13</sup> Along with chemical methods, such as chemical reduction, for the preparation of nanomaterials, biosynthesis using plant extracts is environmentally friendly and cost effective method.<sup>14,15</sup> This synthesis route can be used as an economical and viable alternative for the large-scale production of metal nanoparticles. Raut *et al.*<sup>16</sup> synthesized platinum and palladium metal nanoparticles by rapid biosynthesis using root extract of *Asparagus racemosus* Linn under the sunlight. They

reported that metal nanoparticles formed by bioreduction in an aqueous medium are crystalline in nature and spherical in shape with particle size ranging between 1 to 6 nm. Farhadi *et al.*<sup>17</sup> reported a biogenic process for fabrication of highly dispersed palladium nanoparticles using aqueous extract of *Astraglmanna*, a non-toxic and eco-friendly material, without extra surfactant, capping agent, and template. The mean size of the biosynthesized nanoparticles was found to be approximately 15 nm usage TEM analysis.

As far as we know some efforts have been made on the preparation of PPy-Pd nanocomposite. Fujii *et al.*<sup>18</sup> suggested that PdCl<sub>2</sub>, which act both as an oxidant and as a source of metal atoms, has an efficient oxidant role for pyrrole to form PPy-Pd composite in aqueous media. More recently, Vasilyeva *et al.*<sup>19</sup> illustrated the synthesis of PPy-Pd nanocomposite by direct redox reaction between Pd (II) acetate and pyrrole in acetonitrile. Hamasaki *et al.*<sup>20</sup> synthesized sterically stabilized PPy-Pd nanocomposite particles by aqueous chemical oxidative dispersion polymerization. They reported that PPy-Pd nanocomposite successfully obtained as colloiddally stable aqueous dispersions, which were stable at least for 7 months, using poly(4-lithium styrene sulfonic acid) colloidal stabilizer. They also verified that the average diameters of resulted PPy-Pd nanocomposite particles were approximately 30 nm.

Strong electronic interaction between nanoparticles that incorporate in conducting polymer matrix and polymer molecules may be considered as potential candidate for considering in the innovative biomedical applications. Boomi *et al.*<sup>21</sup> fabricated polyaniline/Au-Pd nanocomposite that exhibited interesting antibacterial activity at micro-molar concentration levels. Recently they also synthesized PANI/Pt-Pd nanocomposites and observed that nanocomposite containing Pt-Pd nanoparticles has good antibacterial activity against *Streptococcus sp* (MTCC 890), *Staphylococcus sp* (MTCC 96), *E. coli* (MTCC 1671) and *Klebsiella sp* (MTCC 7407).<sup>22</sup>

In continuation of our research works on microemulsion systems as soft template for nanomaterial synthesis,<sup>23-27</sup> the aim of this work is preparation of tubular-structured of PPy-Pd nanocomposite using a special microemulsion system. Jang *et al.*<sup>28</sup> reported a new method based on microemulsion templates for fabrication of PPy nanotubes for the first time. They also introduced a mechanism for constructing of conducting polypyrrole nanotubes in reverse micelle system. They showed that AOT reverse cylindrical micelles could be spontaneously formed in an apolar solvent through a cooperative interaction between aqueous FeCl<sub>3</sub> solution and AOT. We used this microemulsion route in this paper to report a simplistic method for the synthesis of PPy-Pd nanocomposite by in situ chemical oxidative polymerization for the first time. In

this method first the bioreduction of palladium by rosemary extract in W/O microemulsion system at room temperature was carried out and AOT reverse cylindrical micelles was formed when an aqueous FeCl<sub>3</sub> solution as oxidant agent was added. After that the pyrrole monomer was added to the blend of previous microemulsion system. The monomers rapidly polymerized by iron cations along the surface of the reverse cylindrical micelles. The resulted PPy-Pd nanocomposite was characterized by FT-IR, XRD, SEM and TEM analysis. Finally as an application, the antibacterial activity of the synthesized nanotube PPy-Pd composite against clinical strain of Gram-positive (*Bacillus* and *Staphylococcus aureus*) and Gram-negative (*Escherichia coli* and *Klebsiella*) bacteria was tested and discussed.

## 2. Experimental

### 2.1. Materials

The anionic surfactant AOT was purchased from Acros Company and used without further purification. Pyrrole monomer (>99%), which was distilled under reduced pressure before using, n-hexane and N-methyl-2-pyrrolidone (NMP) were obtained from Merck. All other reagents including palladium dichloride (PdCl<sub>2</sub>) as source of metal, ferric chloride (FeCl<sub>3</sub>) as oxidizing agent, hydrochloric acid (HCl) for enhancement solubility of PdCl<sub>2</sub> were also obtained from Merck and used as received. Rosemary extract as reducing agent was

prepared in our lab freshly before using. All aqueous solutions were prepared with deionized water.

## 2.2. Synthesis of PPy-Pd composite nanotubes

### 2.2.1. Biosynthesis of stable colloidal Pd nanoparticles in W/O microemulsion

At the first time, reverse AOT micelles was prepared as follows. A solution of anionic surfactant AOT in n-hexane solvent with concentration of 0.1 M was prepared and certain amount of aqueous PdCl<sub>2</sub> solution (0.01M) by fixing the mole ratio of water to AOT at 4, (W = 4) was added to surfactant solution. The mixture was stirred via constant speed for 1h at room temperature and then a colloidal Pd nanoparticle was formed by chemical reduction method using rosemary extract as reducing agent. The reaction mixture changed rapidly from high transparent orange to dark brown.

### 2.2.2. Synthesis of reverse cylindrical AOT micelles including of Pd nanoparticles

An oxidizing solution of FeCl<sub>3</sub> (0.1 M) was added to the prepared Pd colloidal solution. A transparent system was obtained which is consist of 74.0 wt. % of hexane, 22.4 wt. % of AOT and 3.6 wt. % of aqueous FeCl<sub>3</sub> solution.<sup>28</sup>

### 2.2.3. Synthesis of PPy-Pd composite nanotubes

The amount of 0.7 ml of pyrrole monomer was added to the prepared cylindrical micelles dropwise at 15 °C and a dark green solution was obtained. Pyrrole monomers polymerized by iron cations along the surface of the reverse cylindrical micelles to form nanotube shaped composite, which Pd nanoparticles captured in the wall of the tubes. The obtained black powder PPy-Pd was precipitated and washed with acetone/methanol several times until the residues of AOT and other reagents were removed by thoroughly washing with excessive acetone and then dried under vacuum at 60 °C for 24 h. Pure PPy nanotubes was synthesized similar to above route but in absent of PdCl<sub>2</sub> solution and rosemary extract.<sup>28</sup> A feasible mechanism for the formation of the PPy-Pd composite nanotubes and a picture from reaction mixtures are shown in Fig. 1 and Fig. 2, respectively.

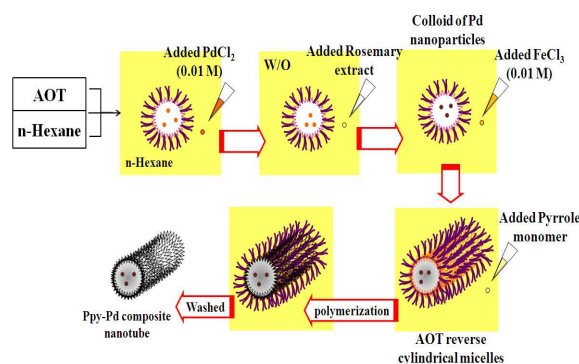


**Fig. 1.** A schematic diagram for the formation of PPy-Pd composite nanotubes in W/O microemulsion template.



**Fig. 2.** Photograph of the reaction mixtures showing color change (a) Rosemary extract (b) Microemulsion including Pd ions (c) Stable colloid Pd nanoparticles prepared in W/O microemulsion (d) Reverse cylindrical AOT micelles including of Pd nanoparticles which pyrrole monomer polymerized along the surface of the reverse cylindrical micelles (e) Resulted PPy-Pd composite nanotubes.

### 2.3. Characterization of PPy-Pd composite nanotubes

The infrared spectra of the PPy and PPy-Pd composite nanotubes were taken as KBr pellets on a Galaxy series FT-IR 5000 spectrophotometer (unicam Co.) in the range 400–4000  $\text{cm}^{-1}$ .

The structure of the PPy and PPy-Pd composite nanotubes were studied by X-ray diffraction (XRD) experiments. A Philips model PW 1800 diffractometer instrument with Cu K $\alpha$  radiation and Ni filter was used to collect the X-ray data. The average crystallite size from a sharp peak is estimated by using the following Scherrer's formula:

$$D = K \lambda / \beta \cos \theta \quad (1)$$

Where  $D$  is the crystallite size,  $K$  is the shape factor, which can be assigned a value of 0.89,  $\theta$  is the diffraction angle at maximum peak intensity, and  $\beta$  is the full width at half maximum of diffraction angle in radians.

The resulted PPy-Pd nanocomposite was characterized by scanning electron microscope (SEM) analysis (LEO 1455VP). SEM photograph, presented in supporting materials (Fig. S1), confirms that PPy-Pd composite is as nanotube shaped.

The surface morphology of PPy-Pd composite nanotubes was observed using a transmission electron microscope (TEM) (Zeiss- EM10C-80KV). Prior to being loaded into the TEM, the sample was made by grinding using mortar and pestle, dispersed in ethanol, sonicated, and dropped into a wholly carbon-coated copper grid.

### 2.4. Antibacterial activity test

#### 2.4.1. Kirby-bauer method

The produced PPy-Pd composite nanotubes and pure PPy were evaluated for antibacterial activity. Agar well diffusion method,<sup>29</sup> was used and the pH was adjusted at 7.3. Clinical isolates of *Bacillus*, *Staphylococcus aureus* (from Gram-positive bacteria), *Escherichia coli* and *Klebsiella spp.* bacteria (from Gram-negative) were selected for this study. Briefly, sterile molten Mueller-Hinton agar (20 ml) was poured into sterile petri dishes and allowed to solidify

at room temperature. Pure cultures of pathogenic bacteria as 0.5 McFarland ( $10^8$  CFU/ml) was swabbed on the Muller-Hinton agar plates. Further 100 mg/ml of N-methyl-2-pyrrolidone dissolved solution of pure PPy and PPy-Pd composite nanotubes were impregnated onto 5 mm paper disk on the inoculated surface of Mueller-Hinton agar plates. Inoculated plates were incubated for 24 h at 37 °C in an incubator. The zone of inhibition was measured and the results were expressed as mm compared to control NMP solution.

#### 2.4.2. Micro-plate Dilution Method

The antibacterial study was accomplished by determining of Minimal Inhibitory Concentration (MIC) and Minimal Bactericidal Concentration (MBC) values of N-methyl-2-pyrrolidone dissolved solution of pure PPy and PPy-Pd composite nanotubes with different concentrations (185, 92.15, 46.25, 23.12, 11.56, 5.78, 2.89, 1.44, 0.72 and 0.36 mg/ml) in 1-10 wells, respectively. In this method, positive control (culture medium containing bacterium and without antibacterial material) and negative control (antibacterial material with culture medium without any bacteria) were in 11 and 12 wells, respectively. MIC and MBC was performed in the same plate using the substrate 3-(4, 5- dimethylthiazol-2-yl)-2,5-diphenyl tetrazolium bromide (MTT). Briefly, the MIC and MBC tests were conducted on sterile 96-well plate using broth micro-dilution method by

serial concentrations of test materials. In this procedure, 100 micro liters of bacterial solution containing  $1.5 \times 10^8$  CFU/ml of Mueller Hinton Broth medium was added to each wells of the 96-well plate. Twenty micro liters of a solution containing 5 mg of MTT in 1 ml of PBS (Phosphate Buffered Saline) was added to each well. The plates were incubated for 90 minutes at 37°C. After that, the MTT solution was carefully excluded from each well. Then, 100  $\mu$ l of DMSO (Dimethyl Sulfoxide) was added to each well to dissolve the sediment containing formazan crystals. The plates were shaken for ten minutes at room temperature and their absorption read at 550 nm wavelengths by an ELISA Reader (Stat Fax 2100).

### 3. Results and Discussion

#### 3.1. X-ray diffraction (XRD) results

In order to confirm the presence of Pd component in the prepared nanocomposite, XRD studies were carried out. The XRD pattern for pure PPy nanotubes in Fig. 3, shows that the PPy powder is amorphous in nature and a broad peak, which observed at about  $2\theta = 24^\circ$ , may be due to the scattering from PPy chains at the interplanar spacing.<sup>30,31</sup> As can be seen in Fig. 3 the PPy-Pd composite nanotubes powder show four peaks at  $38.5^\circ$ ,  $45.1^\circ$ ,  $67.4^\circ$  and  $82.1^\circ$ , which correspond to the (111), (200), (220) and (311) lattice plane diffractions of Pd crystals. These clearly observed peaks are corresponding to the face-centered cubic (fcc) structure of

crystalline Pd in PPy-Pd nanocomposite. The average crystallite size of Pd was calculated using the full width at half maximum of the X-ray diffraction peaks at  $2\theta = 38.5^\circ$  corresponding to the most intense using Eq. 1. The crystallite size of Pd in PPy-Pd composite nanotubes was obtained about 20 nm.

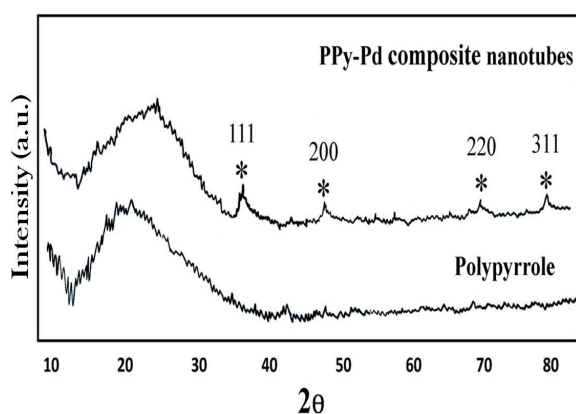


**Fig. 3.** XRD images of PPy and PPy-Pd composite nanotubes.

### 3.2. FT-IR spectroscopy results

The synthesis of pure PPy and PPy-Pd composite nanotubes were monitored by FT-IR spectrometry (Fig. 4). The FT-IR spectrum of pure PPy and PPy-Pd composite nanotubes clearly show the characteristic bands attributable to the =C–H in-plane deformation vibration at  $1049\text{ cm}^{-1}$  and C–C asymmetric stretching vibration at  $1458\text{ cm}^{-1}$ . The main band at  $1609\text{ cm}^{-1}$  is due to the ring-stretching mode of Py ring. The band at  $3434\text{ cm}^{-1}$  is attributed to the N–H stretch vibration and a couple of bands at  $2930$  and  $2874\text{ cm}^{-1}$  are assigned to the C–H stretching vibration.<sup>32</sup> The

broad resonance peak at  $1219\text{ cm}^{-1}$  is assigned to sulfonic group of AOT surfactant.<sup>26</sup> As there is any characteristic band for Pd in FT-IR spectrum of PPy-Pd composite, it can be concluded that the Pd nanoparticles are incorporated into the PPy backbone.

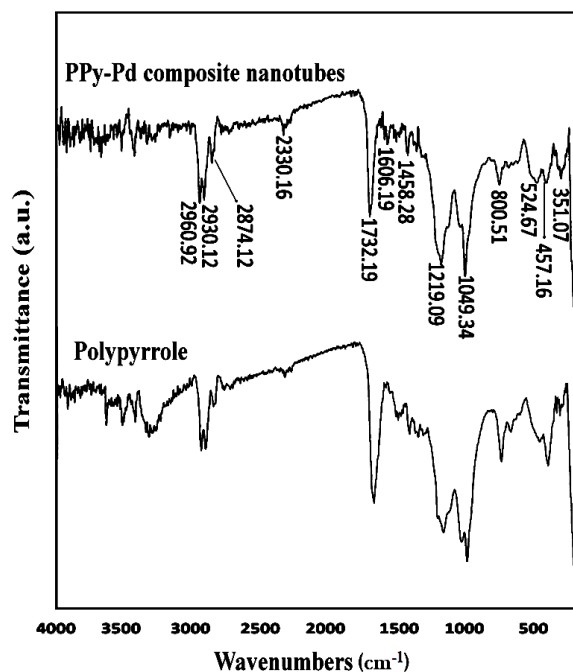


**Fig. 4.** FT-IR spectra of PPy and PPy-Pd composite nanotubes.

### 3.3. SEM and TEM Micrographs

SEM micrograph of the nanocomposite sample (Fig.S1) clearly shows nanotube shape of the polymer. This photograph confirms previous observation of Jang *et al.*<sup>28</sup> which obtained by FE-SEM.

Transmission electron microscopy of PPy-Pd composite nanotubes is shown in Fig. 5. An average diameter of 21.5 nm for Pd nanoparticles trapped in the nanotubes wall was

calculated by using Leica image analyzer. It is confirmed that, reversed microemulsions as a soft template method,<sup>2,33,34</sup> has excellent potential for generating conductive-polymer-metal composite with nanotubular structured by interfacial reactions. Additionally, an image of nanotube shaped PPy-Pd composite with different zoom (scale bare of 400 nm) is presented as inset in Fig. 5.

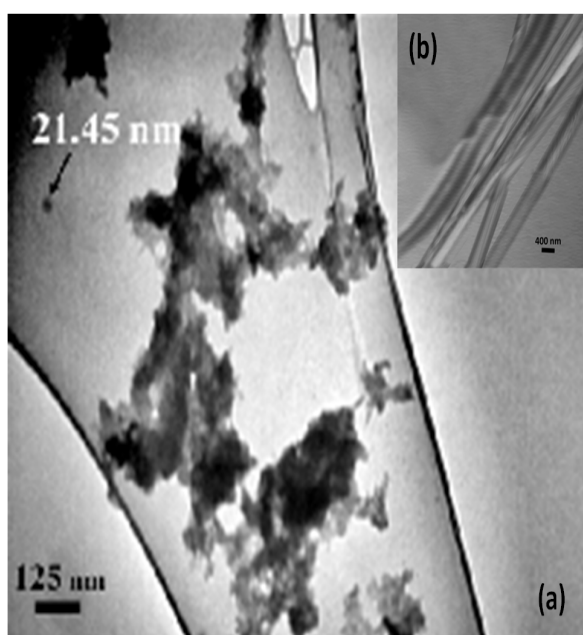


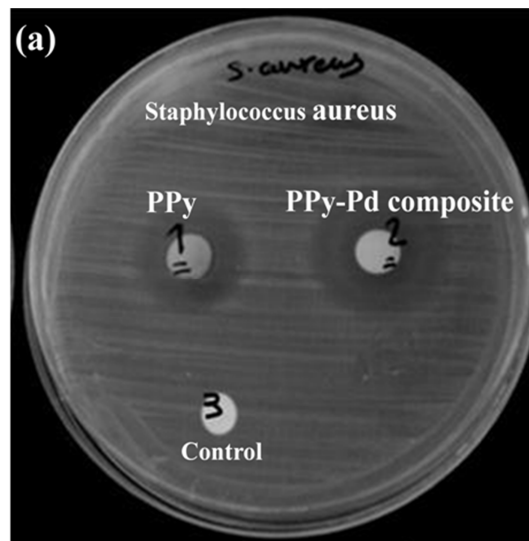
**Fig. 5.** TEM image of PPy-Pd composite nanotubes, (a) scale bare of 125 nm and (b) scale bare 400 nm.

### 3.4. Antibacterial activity results

#### 3.4.1. Results of Kirby-bauer method

The zone of inhibition toward clinical isolates (*Bacillus*, *Staphylococcus aureus*, *Escherichia coli* and *Klebsiella spp.*) with pure PPy and PPy-Pd composite nanotubes was evaluated. As excellent result PPy-Pd composite nanotubes has broad spectrum antibacterial activity. The

data shows that PPy-Pd composite exhibited the highest antibacterial activity against all tested bacteria than pure PPy. The determined zones of inhibition with pure PPy samples were  $16 \pm 0.5$ ,  $0.0$ ,  $6 \pm 0.5$  and  $7 \pm 0.2$  for *Staphylococcus aureus*, *Bacillus spp.*, *Escherichia coli* and *Klebsiella*, respectively. While, the determined zone of inhibition with PPy-Pd composite nanotubes samples were  $23 \pm 0.5$ ,  $10 \pm 0.25$ ,  $16 \pm 0.3$  and  $14 \pm 0.6$  for *Staphylococcus aureus*, *Bacillus spp.*, *Escherichia coli* and *Klebsiella*, respectively. Fig. 6-a shows the zone of inhibition against *Staphylococcus aureus* as an example of Kirby-bauer method. The zone of inhibition toward other clinical isolates bacteria are illustrated in supporting material (S2).



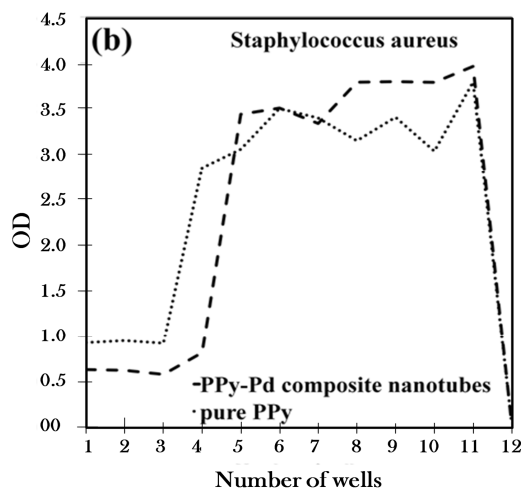


**Fig. 6.** (a) Antibacterial activity of clinical strain of *Staphylococcus aureus*, with (1) Pure PPy, (2) PPy-Pd composite and (3) Control, by Kirby-bauer method. (b) Optical Density (OD) results versus various concentrations of pure PPy and PPy-Pd composite nanotubes by micro-plate dilution method determining MBC for clinical strain of *Staphylococcus aureus*.

#### 3.4.2. Micro-dilution Assay

Among the bacterial strains tested for antibacterial activity, the *Staphylococcus aureus* showed excellent response toward the materials tested than others species. Hence, *Staphylococcus aureus* strain was studied further for MIC and MBC methods. The MIC and MBC results revealed that the PPy-Pd composite nanotubes have excellent effect than pure PPy. The pure PPy exhibited low antibacterial activity against *Staphylococcus aureus*. The MIC values for *Staphylococcus aureus* were obtained as 11.56 and 5.78 mg/ml by PPy and PPy-pd composite nanotubes respectively (Fig. 6-b). The results of the optical

density (OD) measurement using micro-plate dilution method for determination of MBC by the pure PPy and PPy-Pd composite nanotubes toward *Staphylococcus aureus* presented in Fig. 6-b. The existence of low antibacterial activity for pure PPy<sup>35-38</sup> is due to key factors such as electrostatic adsorption between PPy and bacteria, higher molecular weight, surface hydrophilicity and direct contact between polymer and bacteria cell. The MBC results for *Staphylococcus aureus* showed the damage of cells in 46.25 and 23.12 mg/ml by PPy and PPy-pd composite nanotubes respectively (Fig. 6-b). The result confirmed the damage of *Staphylococcus aureus* bacterium. In concentration of 46.25 for pure PPy and 23.12 mg/ml for PPy-Pd *Staphylococcus aureus* could be growth and produced formazan crystals. It's proved the antibacterial material concentration was under bactericidal concentration and the bacterium remained survived. Other wells show similar situation. It was proposed that the nanocomposite may contact to the bacterial membrane and cell wall, and disturb its permeability. It could be causing damage by interacting with phosphorus and sulphur containing compounds such as DNA and protein.<sup>39</sup> As an excellent result the PPy-Pd composite nanotubes with monodispersed Pd nanoparticles have improved antibacterial activity than pure PPy.

#### 4. Conclusion

In this research work after synthesizing Pd nanoparticles in a microemulsion system by using rosemary extract, reverse cylindrical micelles were formed via a cooperative interaction between an aqueous FeCl<sub>3</sub> solution and surfactant. Pyrrole monomers rapidly polymerized by iron cations along the surface of reverse cylindrical micelles. The produced novel nanotubes shaped polypyrrole-Pd composite was studied using different characterization techniques such as FT-IR, XRD and TEM. The synthesized nanocomposite was evaluated for antibacterial activity. The prepared composite has got enhanced antibacterial activity against model organisms, a selective Gram-positive (*Streptococcus sp* and *Staphylococcus sp*) and Gram-negative (*Escherichia coli* and *Klebsiella sp*) bacteria, when compared to pure polypyrrole due to existence of Pd nanoparticles. This is an interesting report on the antibacterial effect of nanotube-shaped PPy-Pd composite and may be investigated as potential candidate for request in futuristic biomedical fields.

#### Acknowledgment

Financial support from the Arak University research group is gratefully acknowledged (Grant No. 90-13897).

#### References

1. S. Liu, H. Xu, J. Ou, Z. Li, S. Yang and J. Wang, *Mater. Chem. Chem. Phys.*, 2012, **132**, 500.
2. M. Choudhary, R. Ul Islam, M. J. Witcomb and K. Mallick, *Dalton Trans.*, 2014, **43**, 6396.
3. F. Hu, W. Li, J. Zhang and W. Meng, *J. Mater. Sci. Tech.*, 2014, **30**, 321.
4. M. Joulazadeh, A. H and Navarchian, *Synthetic Met.*, 2015, **199**, 37.
5. C. Li, W. Cai, C. Kan and G. Fu, *Sci. Mater.*, 2004, **50**, 1481.
6. C. J. Murphy, T. K. Sau, A. M. Gole, C. J. Orendorff, J. Gao, L. Gou, S. E. Hunyadi and T. Li, *J. Phys. Chem. B*, 2005, **109**, 13857.
7. L. M. Liz-Marzan, *Langmuir*, 2006, **22**, 32.
8. W. P. McConnell, J. P. Novak, L. C. Brousseau, R. R. Fuierer, R. C. Tenent and D. L. Feldheim, *J. Phys. Chem. B*, 2000, **104**, 8925.
9. W. Tu, K. Fukui, A. Miyazaki and T. Enoki, *J. Phys. Chem. B*, 2006, **110**, 20895.
10. W. Zhang, Q. Ge and L. Wang, *J. Chem. Phys.*, 2003, **118**, 5793.
11. F. Xie, J. Hu, C. Jin and Q. Wang, *J. Exp. Nanosci.*, 2013, **8**, 825.
12. X. Chu, D. Duan, G. Shen and R. Yu, *Talanta*, 2007, **71**, 2040.
13. Y. Teow and S. Valiyaveetil, *Nanoscale*, 2010, **2**, 2607.
14. A. K. Jha, K. Prasad and A. R. Kulkarni, *Colloid Surf. B Biointerfaces*, 2009, **73**, 219.
15. K. S. Kavitha, S. Baker, D. Rakshith, H. U. Kavitha, R. H. C. Yashwantha and B. P. Harini,

- S. Satish, *Int. Res. J. Biological Sci.*, 2013, **2**, 66.
16. R. W. Raut, A.S. M. Haroon, Y. S. Malghe, B. T. Nikam and S. B. Kashid, *Adv. Mater. Lett.* 2013, **4**, 650.
17. K. Farhadi, A. Pourhossein, M. Forough, R. Molaie, A. Abdi and A. Siyami, *J. Chin. Chem. Soc.*, 2013, **60**, 1144.
18. S. Fujii, S. Matsuzawa, Y. Nakamura, A. Ohtaka, T. Teratani, K. Akamatsu, T. Tsuruoka and H. Nawafune, *Langmuir*, 2010, **26**, 6230.
19. S. V. Vasilyeva, M. A. Vorotyntsev, I. Bezverkhyy, E. Lesniewska, O. Heintz and R. Chassagnon, *J. Phys. Chem. C*, 2008, **112**, 19878.
20. H. Hamasaki, N. Fukui, S. Fujii, S. I. Yusa and Y. Nakamura, *Colloid Polym. Sci.*, 2013, **291**, 223.
21. P. Boomi and H. G. Prabu, *Colloid Surf. A*, 2013, **429**, 51.
22. P. Boomi, H. G. Prabu and J. Mathiyarasu, *Eur. J. Med. Chem.*, 2014, **72**, 18.
23. F. Mirhoseini and A. Salabat, *RSC Adv.*, (DOI: 10.1039/C4RA14612C).
24. A. Salabat A and M. Rahmati Far, *Russ. J. Phys. Chem. A*, 2012, **86**, 881.
25. A. Salabat and H. Saydi, *Russ. J. Phys. Chem. A*, 2012, **86**, 2014.
26. A. Salabat and H. Saydi, *Polym. Composites*, 2014, **35**, 2023.
27. S. Soleimani, A. Salabat and R. F. Tabor, *J. Colloid Interface Sci.*, 2014, **426**, 287.
28. J. Jang and H. Yoon, *Langmuir*, 2005, **21**, 11484.
29. A. Shirley, B. Dayanand, B. Sreedhar and S. G. Dastager, *Dig. J. Nanomater. Bios.*, 2010, **5**, 447.
30. R. Partch, S. G. Gangolli, E. Matijevic, W. CaL and S. Araj, *J. Colloid Interface Sci.*, 1991, **144**, 27.
31. J. Y. Ouyang and Y. F. Li, *Polymer*, 1997, **38**, 3997.
32. C. Jeyabharathi, P. Venkateshkumar, J. Mathiyarasu and K. L. N. Phani, *J. Electrochem. Soc.* 2010, **157**, B1740.
33. L. Pan, H. Qiu, C. H. Dou, Y. Li, L. Pu, J. Xu and Y. Shi, *Int. J. Mol. Sci.*, 2010, **11**, 2636.
34. Z. X. Wei, L. J. Zhang, M. Yu, Y.S. Yang and M. X. Wan, *Adv. Mater.*, 2013, **15**, 1382.
35. P. K. Prabhakar, S. Raj, P. R. Anuradha, S. N. Sawant and M. Doble, *Colloids Surf.*, 2011, **86**, 146.
36. X. Liang, M. Sun, L. Li, R. Qiao, K. Chen, Q. Xiao and F. Xu, *Dalton Trans.*, 2012, **41**, 2804.
37. N. P. S. Chauhan, R. Ameta and S. C. Ameta, *J. Indian Counc. Chem.*, 2010, **27**, 128.
38. H. Zuo, D. Wu and R. Fu, *J. Appl. Polym. Sci.*, 2012, **125**, 3537.
39. M. S. Tamboli, M. V. Kulkarni, R. H. Patil, W. N. Gade, S. H. C. Navale and B. B. Kale, *Colloid Surf. B*, 2012, **92**, 35.